Materials Chemistry and Physics 118 (2009) 398–404

Contents lists available at ScienceDirect

Materials Chemistry and Physics

journal homepage: www.elsevier.com/locate/matchemphys

Morphology evolution of polysulfone nanofibrous membranes toughened epoxy resin during reaction-induced phase separation

Gang Li[a], Zhibin Huang[b], Chunling Xin[a], Peng Li[b], Xiaolong Jia[b], Binghui Wang[b], Yadong He[a,*], Seungkon Ryu[c], Xiaoping Yang[b,*]

[a] College of Mechanical and Electrical Engineering, Beijing University of Chemical Technology, Beijing 100029, PR China
[b] The Key Laboratory of Beijing City on Preparation and Processing of Novel Polymer Materials, Beijing University of Chemical Technology, Beijing 100029, PR China
[c] Department of Chemical Engineering, Chungnan National University, Daejeon 305-764, Republic of Korea

ARTICLE INFO

Article history:
Received 13 March 2009
Received in revised form 25 July 2009
Accepted 4 August 2009

Keywords:
Nanostructures
Phase transitions
Microstructure
X-ray scattering

ABSTRACT

The phase separation process and morphology evolution of 5 wt% polysulfone (PSF) nanofibrous membranes toughened epoxy resin at different temperatures were investigated by synchrotron radiation small angel X-ray scattering (SR-SAXS), phase contrast microscopy (PCM) and scanning electron microscopy (SEM). The onset time of phase separation obtained by different methods was basically identical. As the curing proceeded at constant temperature, the scattering peak corresponding to the maximum scattering intensity shifted to a smaller scattering vector (q_m), and the average diameters of PSF spheres increased, which showed a phase separation pattern of nucleation and growth mechanism. PSF spheres exhibited random alignment in "sea-island" morphology, which was attributed to the in situ phase separation of PSF nanofibers. Also, the effects of phase separation kinetics on the phase morphology and fracture toughness of nanofibrous membranes toughened epoxy resin were investigated. Results showed that the phase separation process was faster than the curing reaction process, which implied that the diffusion coefficient of PSF in epoxy resin increased with increasing the curing temperature, resulting in the increase of PSF sphere size that in turn improved the fracture toughness at higher temperature.

1. Introduction

Polysulfone (PSF) has been widely used to toughen epoxy matrix without the expense of thermal and mechanical properties of thermosetting resins [1–3]. In such systems the toughness improvement was due to the immiscible two-phase structure resulted from reaction-induced phase separation [4–6], whereas the homogeneous phase structure could not improve the toughness of epoxy matrix effectively [7]. In general, reaction-induced phase separation was relating to several transformations: phase separation resulted from the increase in the molecular weight of the original monomer, gelation and/or vitrification of the cross-linked polymer [8,9]. Thus, the morphology evolution of the toughened systems was controlled by two antagonistic effects of phase separation and cross-linking reaction. Specifically, the phase-separated morphology induced by the curing reaction depended on the rates of phase separation and cross-linking reaction [10,11]. The former was activated by the reaction via thermodynamical instabilities, whereas the latter tended to suppress the phase separation by slowing down the polymer chain diffusion [10,12]. The competition between phase separation kinetics and cross-linking reaction kinetics, which were governed by the curing conditions, molecular weights, etc. [13–17], would result in various phase-separated morphologies. Therefore, the studies on the phase separation and morphology evolution during the curing process were beneficial to design polysulfone toughened epoxy with high performance.

In our previous work, PSF nanofibrous membranes have been successfully used in toughening carbon fiber/epoxy composite [18]. The improvement of toughness and the maintenance of modulus were attributed to the inhomogeneous phase structure, and PSF spheres generated from phase separation of nanofibrous membranes exhibited random alignment. However, the morphology evolution of nanofibrous membranes toughened epoxy resins during the reaction-induced phase separation, and the effects of kinetics of phase separation and cross-linking reaction on phase-separated morphology and fracture toughness have not been investigated.

Therefore, in this work, the morphology evolutions of 5 wt% PSF nanofibrous membranes toughened epoxy resin were investigated by using various techniques during reaction-induced phase separation at different curing temperatures. Synchrotron radiation small angel X-ray scattering (SR-SAXS) was used to trace the evolution of the maximum scattering intensity and scattering vector q, and the evolutions of phase structure obtained by SR-SAXS were compared

* Corresponding authors.
E-mail address: yangxp@mail.buct.edu.cn (X. Yang).

0254-0584/$ – see front matter © 2009 Elsevier B.V. All rights reserved.
doi:10.1016/j.matchemphys.2009.08.001

to those observed by phase contrast microscopy (PCM) and scanning electron microscopy (SEM). Differential scanning calorimetry (DSC) was used to obtain the glass transition temperature (T_g) of phase-separated systems and the epoxide conversion at isothermal curing. The effects of the curing temperature on the kinetics of phase separation and cross-linking reaction were investigated. The influences of phase separation on the fracture toughness of nanofibrous membranes toughened epoxy resin were also discussed.

2. Experimental

2.1. Materials

The epoxy resin used in this work was tetraglycidyl 4,4′-diaminodiphenyl methane (TGDDM, AG-80, Shanghai Institute Synthetic Resins Co., China). The hardener used was 4,4′-diaminodiphenyl sulfone (DDS, Yinsheng Chemical Co., Ltd., China). Bisphenol-A polysulfone (PSF, Udel P1700, Amoco Co., USA) was used as a toughener. N,N′-dimethylacetamide (DMAC) and acetone were used as solvents during electrospinning process.

2.2. Preparation of resin mixture and PSF nanofibrous membrane

The epoxy (TGDDM) and hardener (DDS) were mixed with a weight ratio of 100:30 by vigorous stirring at 130 °C for 30 min, and the blend was degassed under vacuum to obtain homogeneous resin mixture.

Polysulfone (PSF) solution was prepared by dissolving 25.0 g polysulfone pellets in 90.0 ml N,N′-dimethylacetamide (DMAC) and 10.0 ml acetone. This solution was transferred to a 20 ml medical syringe, and electrospun to fabricate PSF nanofibrous membranes at a flow rate of 1.5 ml h^{-1} under 24 kV voltages, following our previous work [18].

2.3. Analyses

2.3.1. Synchrotron radiation small angel X-ray scattering (SR-SAXS)

PSF nanofibrous membranes (5 wt%) and resin mixture (95 wt%) were sandwiched between two polytetrafluoroethylene (PTFE) films (thickness 50 μm) to prepare the samples for SR-SAXS. A set of these samples was isothermally cured at 180, 190, and 200 °C, respectively in a temperature controlled oven. Then, at different time interval, a corresponding sample was removed and quenched by liquid nitrogen. SR-SAXS analyses were performed at the Beijing Synchrotron Radiation Facility. The wavelength of incident X-rays was 0.154 nm, and the camera length was 1830 nm. The change in the light-scattering profiles of the prepared samples was recorded.

2.3.2. Phase contrast microscopy (PCM)

The resin mixture was dropped onto PSF nanofibrous membranes on a glass slide; subsequently it was covered with another glass slide and held together with clamps. The content of nanofibrous membranes was adjusted to 5 wt%. A set of these samples was isothermally cured at 180, 190, and 200 °C, respectively in a temperature controlled oven. At different time interval, partially cured sample was removed and quenched by liquid nitrogen. The morphology evolutions were observed with Nikon inverted microscopy (TE 2000, Japan). The average diameter of PSF phase was obtained using the software of PCM micrographs (Image J).

2.3.3. Scanning electron microscopy (SEM)

Morphology evolutions of the samples used in PCM observations, which were cured for 50 min at 180 °C, 45 min at 190 °C, and 30 min at 200 °C, respectively, were also observed with scanning electron microscopy (SEM, HITACHI S4700, Japan). The surfaces of all samples were coated with a thin layer of a gold alloy. The average diameters of PSF spheres were measured using software of SEM images (Image J).

2.3.4. Differential scanning calorimetry (DSC)

A differential scanning calorimeter (DSC, Perkin-Elmer, PYRIS 1) was used for the isothermal curing of PSF nanofibrous membranes toughened epoxy resin and measurement of the glass transition temperature (T_g). The 5 wt% nanofibrous membranes toughened epoxy resin (3–5 mg) were sealed in aluminium pans, and isothermally cured at 180, 190, and 200 °C for different time interval. Then the samples were quenched by liquid nitrogen to −50 °C, and dynamically scanned to 200 °C at 20 °C min^{-1}. The temperature at 1/2 ΔC_p in the heat flow curves was assigned as the T_g.

The reaction heat, ΔH_t, of the 5 wt% PSF nanofibrous membranes toughened epoxy resin (5–8 mg), was measured at 180, 190, and 200 °C, respectively. After the isothermal curing measurements, the samples were scanned again at 10 °C min^{-1} to obtain the residual heat, ΔH_r. The epoxide conversion, α, was calculated using Eq. (1) [13]:

$$\alpha = \frac{\Delta H_t}{\Delta H_t + \Delta H_r} \quad (1)$$

2.4. Measurement of fracture toughness

The resin casts of resin mixture and 5 wt% PSF nanofibrous toughened epoxy resin were prepared by curing for 50 min at 180 °C, 45 min at 190 °C, and 30 min at 200 °C, respectively. Prior to testing, the casts were precracked by inserting a thin razor into the machined notch and impacting with a hammer to obtain a natural crack. The fracture toughness (K_{IC}) was measured by tensile testing machine (Instron 1121) with the compact tension method according to ASTM D 5045-99. The crosshead speed was 2 mm min^{-1}.

3. Results and discussion

3.1. Morphology evolutions monitored by SR-SAXS

Fig. 1 shows the scattering intensity versus the scattering vector (q) of 5 wt% PSF nanofibrous toughened epoxy resin cured at 180, 190, and 200 °C as a function of time. The scattering vector (q) is defined by Eq. (2) [8,16,17]:

$$q = \left(\frac{4\pi}{\lambda}\right) \sin\left(\frac{\theta}{2}\right) \quad (2)$$

where λ is the wavelength of the scattering light, and θ is the scattering angle.

No scattering light was observed at the early stage of curing, indicating a miscibility at the used wavelength scale. After a time lag, scattering peaks corresponding to the maximum scattering intensity occurred at a scattering vector (q_m) of 0.0235 nm^{-1} at 180 °C, 0.0226 nm^{-1} at 190 °C, and 0.0214 nm^{-1} at 200 °C, respectively. The results indicated that phase separation was induced by the curing reaction, and the onset time of the phase separation was about 17, 12, and 7 min, respectively. As the curing proceeded, the scattering peak gradually shifted to a smaller scattering vector (q_m), which implied a typical phase separation pattern of nucleation and growth mechanism [19,20].

The characteristic length of nanofibrous membranes toughened epoxy was calculated from the maximum scattering vector (q_m) in Fig. 1 according to Eq. (3) [12,16]:

$$\Lambda_m = \frac{2\pi}{q_m} \quad (3)$$

Fig. 2 shows the characteristic length of 5 wt% PSF nanofibrous membranes toughened epoxy resin cured at 180, 190, and 200 °C, respectively. The characteristic length increased with the increase of curing time at constant temperature. At three temperatures, the characteristic length increased from 267 nm at 17 min to 455 nm at 50 min, from 278 nm at 12 min to 487 nm at 45 min, from 299 nm at 7 min to 506 nm at 30 min, respectively. With increasing the curing temperature, larger size PSF spheres were obtained, which suggested that the higher curing temperature was favorable to the further development of phase separation in this system.

3.2. Morphology evolutions observed by PCM

Figs. 3–5 show the morphology evolutions observed with PCM as increasing the time in 5 wt% PSF nanofibrous membranes toughened epoxy resin cured at 180, 190, and 200 °C, respectively. Dark areas corresponded to epoxy-rich phase, whereas clear domains indicated PSF-rich phase. As displayed in Fig. 3(a), the nanofibers were initially dissolved in epoxy matrix at high temperature, and dissolved completely within 15 min, shown in Fig. 3(b), which implied that the excellent compatibility between nanofibrous membranes and epoxy resins resulted in a homogeneous solution. With the curing reaction proceeding, clear domains of PSF spheres resulted from the phase separation began to appear in epoxy matrix, exhibiting sea-island phase structure, shown in Fig. 3(c). The result indicated that the onset time of phase separation was approximately at 18 min. As curing proceeded, PSF spheres grew in

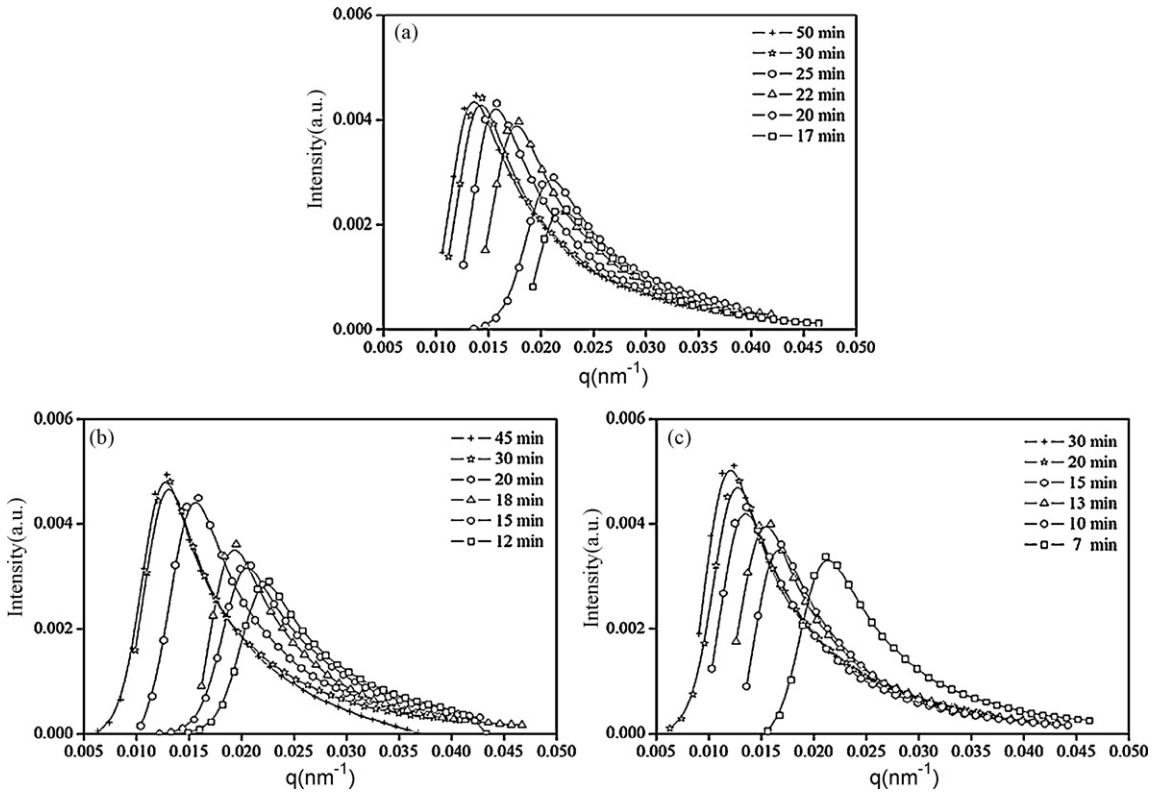

Fig. 1. Scattering intensity versus scattering vector of PSF nanofibrous membranes toughened epoxy resin cured at (a) 180 °C, (b) 190 °C, and (c) 200 °C as a function of time.

size due to the coalescence and ripening, and the average diameter increased to 428 nm, shown in Fig. 3(d), which showed that the phase separation followed a typical nucleation and growth mechanism [20,21].

With increasing the curing temperature, the size of PSF spheres increased and the number of dispersed spheres decreased, as shown in Figs. 4 and 5. The average diameters of PSF spheres were increased to 493 nm at 190 °C and 525 nm at 200 °C. The enlargement of PSF spheres was attributed to the increase in the cross-linking reaction rate and the reduction in viscosity at the beginning of phase separation [22], which started from 12 and 8 min at 190 and 200 °C, respectively. The results were consistent with the beginning of phase separation monitored by SR-SARX. At higher curing temperature, the enhanced mobility of PSF segments and the decreased compatibility between epoxy and PSF led to the higher phase separation rate in comparison with the curing reaction rate, which resulted in a large extent of phase separation before gelation or vitrification [12,22]. In addition, PSF spheres resulted from reaction-induced phase separation exhibited random alignment, which was generated in situ along the nanofibers direction. The results were coincided with the inhomogeneous toughening mechanisms proved in our previous work [18].

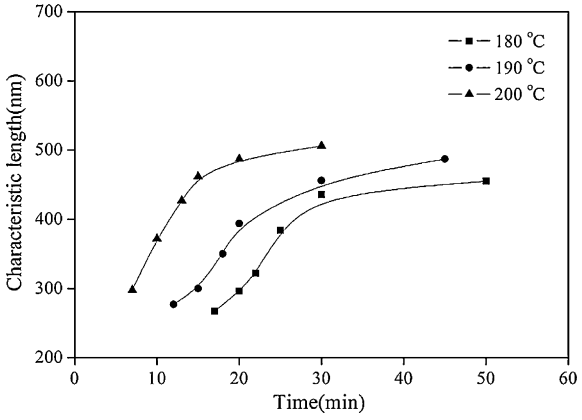

Fig. 2. Characteristic length of PSF nanofibrous membranes toughened epoxy resin cured at (a) 180 °C, (b) 190 °C, and (c) 200 °C as a function of time.

3.3. Morphology evolutions observed by SEM

Fig. 6 shows SEM images of 5 wt% PSF nanofibrous membranes toughened epoxy resin cured for 50 min at 180 °C, 45 min at 190 °C, and 30 min at 200 °C, respectively. Due to the random orientation of the nanofibers in PSF membranes, PSF spheres were also aligned along the nanofiber direction, which was similar to the results observed by PCM. The diameters of PSF spheres demonstrated non-uniform distributions, which were resulted from random junctions of different nanofibers and various PSF concentrations at local regions. The results were in agreement with those of nanofibrous membranes toughened carbon fiber/epoxy composite [18]. The average diameter of PSF spheres obtained from SEM images is compared with those of PCM and SR-SARX analysis, and arranged in Table 1. The average diameters of PSF spheres were 447 nm at 180 °C, 559 nm at 190 °C and 615 nm at 200 °C, respectively. With increasing the curing temperature, the average diameter of PSF spheres increased gradually, which was corresponded with the results obtained from PCM. Also, the average diameter of PSF spheres exhibited the same variable tendency as that of the characteristic length obtained from SR-SARX.

Table 1
Comparison of the results obtained by three characterization techniques.

Temperature (°C)	180	190	200
Time (min)	50	45	30
Characteristic length by SAXS (nm)	455	487	506
Average diameter of PSF spheres by PCM (nm)	428	493	525
Average diameter of PSF spheres by SEM (nm)	447	559	615

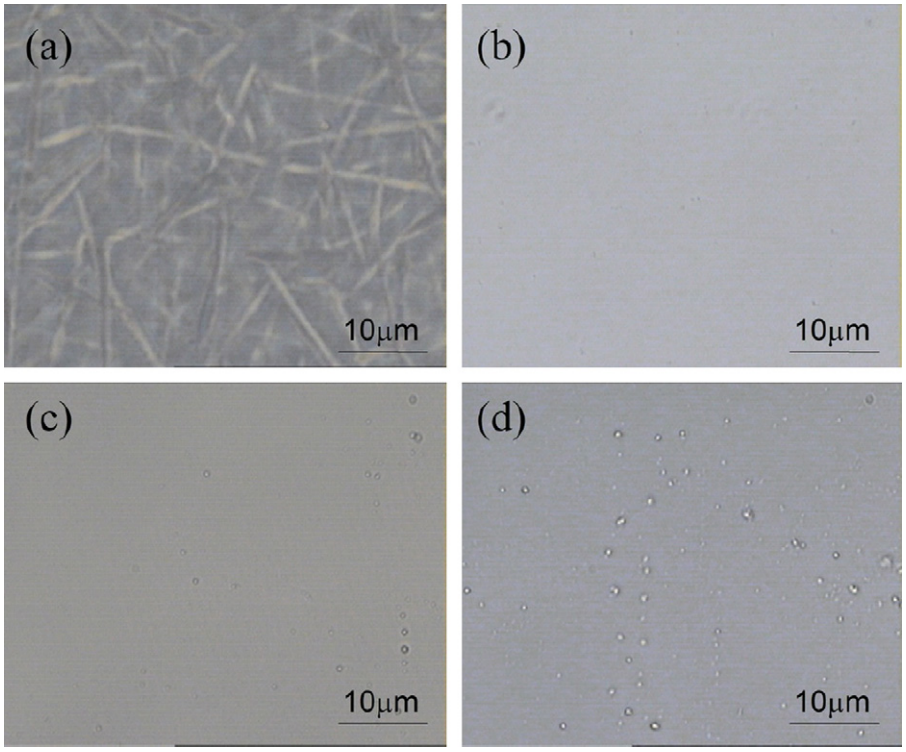

Fig. 3. Morphology evolutions observed by PCM in PSF nanofibrous membranes toughened epoxy resin cured at 180 °C, curing time: (a) 0 min, (b) 15 min, (c) 18 min and (d) 50 min.

3.4. Kinetics of phase separation and cross-linking reaction

PSF nanofibrous membranes toughened epoxy resins were homogeneous in the early stage as observed by PCM, and there existed only one T_g. As the curing proceeded, the mixing entropy decreased with increasing the molecular weight of epoxy resins, while the enthalpy was almost constant due to little change of Flory-Huggins interaction parameter. According to the Flory-Huggins meanfield theory, the homogeneous mixture would be disturbed with the increase of molecular weight of epoxy resins [16,23], which resulted in the occurrence of phase separation that in turn generated two T_g. The transition

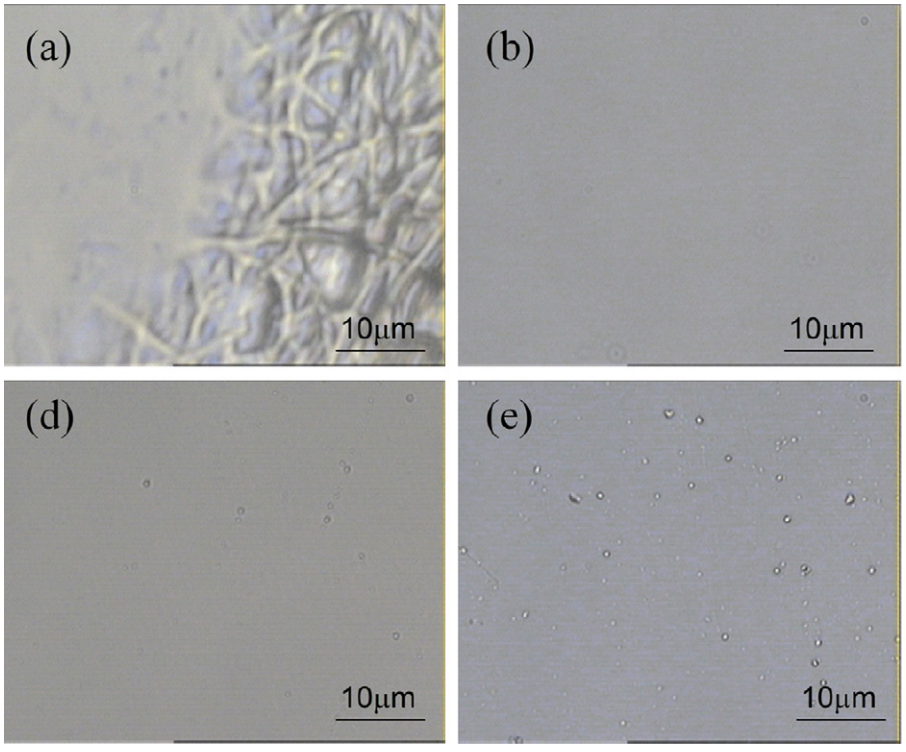

Fig. 4. Morphology evolutions observed by PCM in PSF nanofibrous membranes toughened epoxy resin cured at 190 °C, curing time: (a) 0 min, (b) 10 min, (c) 12 min and (d) 45 min.

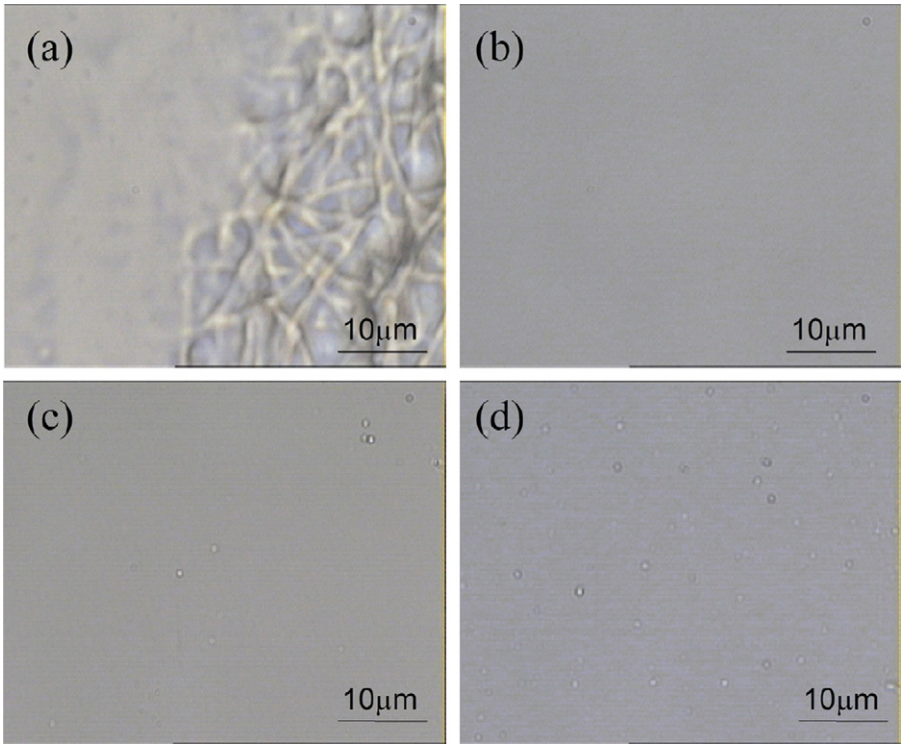

Fig. 5. Morphology evolutions observed by PCM in PSF nanofibrous membranes toughened epoxy resin cured at 200 °C, curing time: (a) 0 min, (b) 5 min, (c) 8 min and (d) 30 min.

from one T_g to two T_gs meant the beginning of phase separation [14,24].

Fig. 7 shows the heat flow curves of 5 wt% PSF nanofibrous membrane toughened epoxy resin cured at 180, 190, and 200 °C as a function of time. The curing times corresponding to the appearance of two T_gs were the onset times of phase separation, which were around 18 min at 180 °C, 13 min at 190 °C, and 8 min at 200 °C, respectively. The results were agreed well with those obtained from SR-SRAX and PCM observations. In addition, after curing for 50 min at 180 °C, 45 min at 190 °C and 30 min at 200 °C, two T_gs of the epoxy-rich phase were much lower than the reaction temperature, which implied that the phase separation was still in progressing, as stated by Wu [12].

When the phase morphology exhibited sea-island structure, with increasing the curing temperature, the size of PSF spheres was mainly depended on the competition between the phase separation rate and the cross-linking reaction rate [19]. The time that gelation occurred during the network formation was usually used to characterize the cross-linking reaction rate. According to the classic Flory-Stockmayer theory, the reaction extent at gelation point, p_{gel}, can be calculated using Eq. (4) [25,26]:

$$p_{gel} = \frac{1}{[r + rs(f-2)]^{1/2}} \tag{4}$$

where f is the functionality of crossing groups, r is the ratio of the epoxide to the amine hydrogen, and s is the fraction of the amine

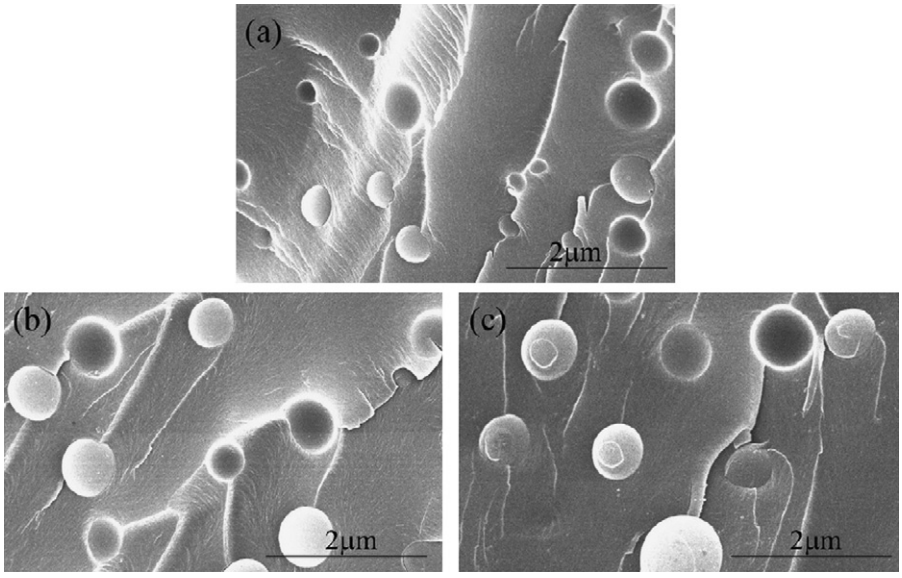

Fig. 6. SEM images of polysulfone nanofibrous membranes toughened epoxy resin cured for (a) 50 min at 180 °C, (b) 45 min at 190 °C, and (c) 30 min at 200 °C.

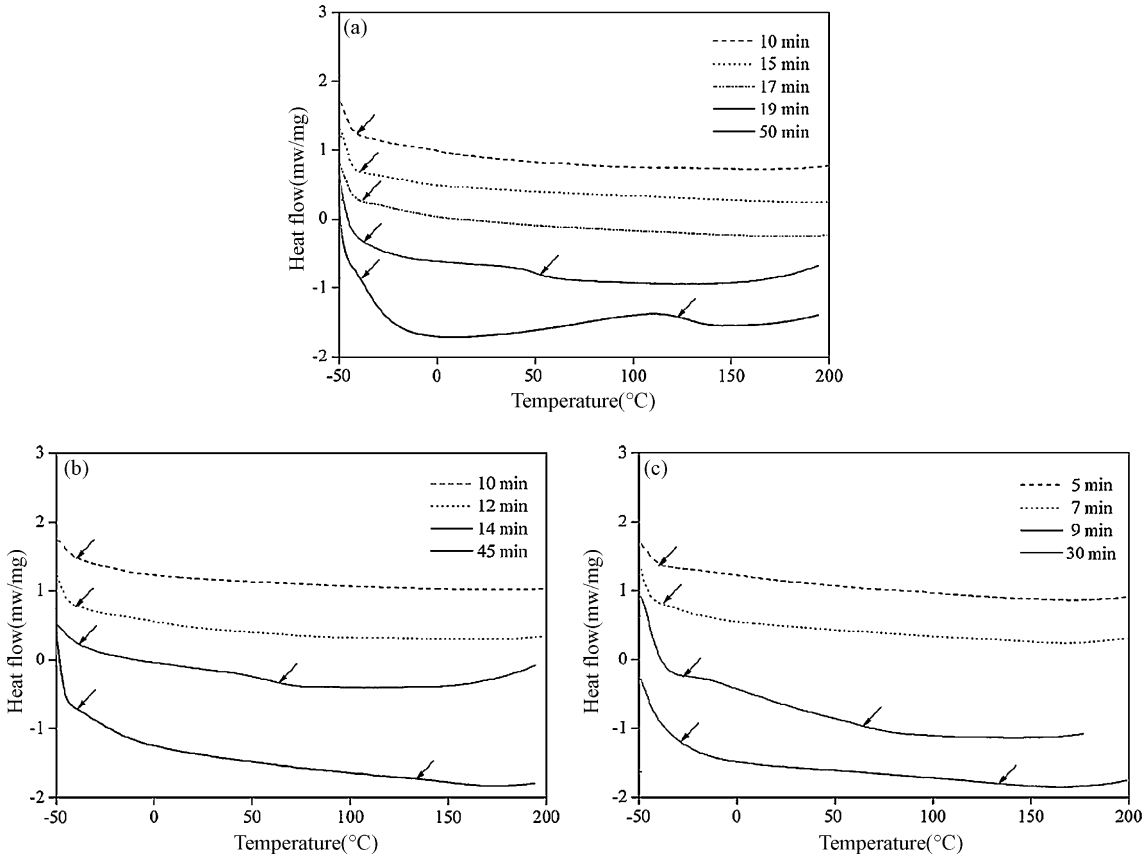

Fig. 7. Heat flow curves of PSF nanofibrous membranes toughened epoxy resin after isothermal curing for various time at (a) 180 °C, (b) 190 °C, and (c) 200 °C.

hydrogen in the multifunctional reactants. For the epoxy/amine reaction in this study, $p_{gel} = 0.32$, which was close to the results of TGDDM/DDS system reported previously [26,27]. In addition, the effects of the primary and secondary amines resulted in a shift of the gel point toward a higher reaction extent by 4% at the most [26,28]. Therefore, the predicted reaction extent at the gel point was in the range of 0.32–0.36.

Fig. 8 shows the epoxide conversion versus time of 5 wt% PSF nanofibrous membranes toughened epoxy resin cured at 180, 190, and 200 °C. The increase of curing temperature accelerated the cross-linking reaction rate and reaction extent, which might shorten the time available for phase separation. At three temperatures, the times arriving to gel points were 23–25, 17–19, and 11–13 min, respectively. The results showed a relatively larger span with respect to the onset time of phase separation aforementioned, which resulted in easy phase separation and fast coalescence of dispersed PSF spheres [29].

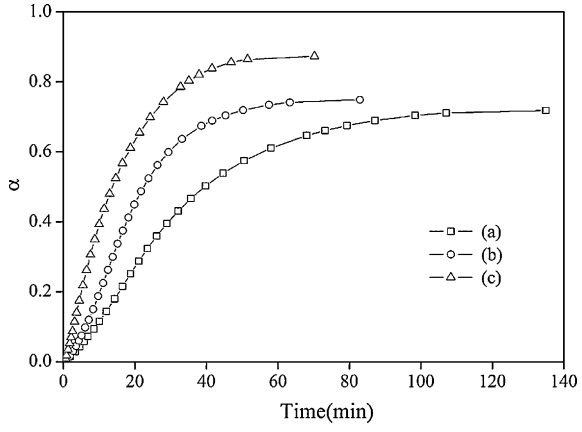

Fig. 8. The epoxide conversion versus time of PSF nanofibrous membranes toughened epoxy resin cured at (a) 180 °C, (b) 190 °C, and (c) 200 °C.

Combined with the analysis of PCM and SEM images, the above results suggested that the phase separation process was faster than the curing reaction process [29]. Therefore, the phase morphology was mainly controlled by the phase separation rate rather than the cross-linking reaction rate. In this case, the diffusion coefficient of PSF in epoxy resins would be the most important factor to affect the phase-separated morphology [19,30]. The increase of the diffusion coefficient resulted from the increase of the curing temperature would lead to increasing the size of PSF spheres.

3.5. Fracture toughness of nanofibrous membranes toughened epoxy

Fig. 9 shows the fracture toughness (K_{IC}) of resin mixture and 5 wt% PSF nanofibrous membranes toughened epoxy resin cured for 50 min at 180 °C, 45 min at 190 °C, and 30 min at 200 °C, respectively. At different temperature, the fracture toughness of nanofibrous membranes toughened epoxy resin was higher than that of resin mixture, which was attributed to the phase separation of PSF. With increasing the temperature, the fracture toughness of nanofibrous membranes toughened epoxy resin increased. The K_{IC} of nanofibrous membranes toughened epoxy cured at 200 °C increased by 42% compared to that cured at 180 °C. In particulate-filled toughened resins, the crack front could be "pinned" easily by the hard particles with random orientation [31]. Also, the rigid particles might result in the deflection of the crack front that in turn generated larger crack-tip-opening displacement [31]. Therefore, as shown in Fig. 6, the dominant toughening mechanism in

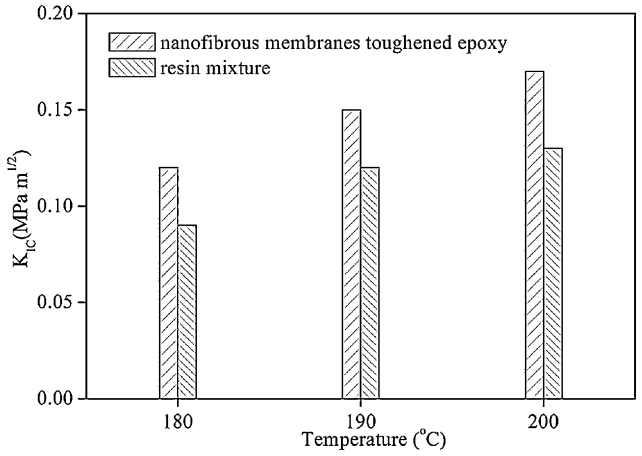

Fig. 9. Fracture toughness (K_{IC}) of resin mixture and 5 wt% PSF nanofibrous membranes toughened epoxy resin cured for (a) 50 min at 180 °C, (b) 45 min at 190 °C, and (c) 30 min at 200 °C.

such systems was crack path deflection and crack pinning. In this case the fracture toughness was strongly dependent on the size of the dispersed particles [32]. At the experimental conditions in our work, the increase of the average diameter of PSF spheres resulted in the improvement of the fracture toughness at higher temperature.

4. Conclusion

During the reaction-induced phase separation of 5 wt% polysulfone nanofibrous membranes toughened epoxy resins, the phase separation followed nucleation and growth mechanism. Accompanied with the morphology evolution, the average diameters of PSF spheres with random alignment increased at constant temperature. The onset time of phase separation obtained from synchrotron radiation small angel X-ray scattering (SR-SAXS) was corresponded well with those from other characterization techniques. With increasing the curing temperature, the size of PSF spheres increased, which was due to the increase of phase separation rate resulted from the increased diffusion coefficient at higher temperature. The increase of PSF sphere size resulted in the improvement of fracture toughness at higher temperature. The results would be helpful to control the phase structure development in nanofibrous membranes toughened composite.

Acknowledgment

The authors would like to thank the National Natural Science Foundation of China for supporting this project (50873010).

References

[1] P. Huang, S. Zheng, J. Huang, Q. Guo, Polymer 38 (1997) 5565.
[2] S. Jin, H.C. Kim, J. Polym. Sci. Polym. Phys. 39 (2001) 121.
[3] E. Girard-Reydet, C.C. Riccardi, H. Sautereau, J.P. Pascault, Macromolecules 28 (1995) 7608.
[4] T. Yoon, B.S. Kim, D.S. Lee, J. Appl. Polym. Sci. 66 (1997) 2233.
[5] P.A. Oyanguren, C.C. Riccardi, R.J.J. Williams, I. Mondragon, J. Polym. Sci. Polym. Phys. 36 (1998) 1349.
[6] R.J. Varley, J.H. Hodgkin, G.P. Simon, Polymer 42 (2001) 3847.
[7] M.C. Chen, D.J. Hourston, W.B. Sun, Eur. Polym. J. 28 (1992) 1471.
[8] N. Mekhilef, H. Verhoogtt, Polymer 37 (1996) 4069.
[9] Z. Zhang, J. Cui, J. Li, K. Sun, W. Fan, Macromol. Chem. Phys. 202 (2001) 126.
[10] A. Harada, Q. Tran-Cong, Macromolecules 30 (1997) 1643.
[11] J. Cui, W. Chen, Z. Zhang, S. Li, Macromol. Chem. Phys. 198 (1997) 1865.
[12] X. Wu, J. Cui, Y. Ding, S. Li, B. Dong, J. Wang, Macromol. Rapid Commun. 22 (2001) 409.
[13] C.C. Su, E.M. Woo, Polymer 36 (1995) 2883.
[14] J. Cui, Y. Yu, S. Li, Macromol. Chem. Phys. 199 (1998) 1645.
[15] I. Martineza, M.D. Martina, A. Eceizaa, P.A. Oyanguren, I. Mondragona, Polymer 41 (2000) 1027.
[16] W. Gan, Y. Yu, M. Wang, Q. Tao, S. Li, Macromol. Rapid Commun. 24 (2003) 952.
[17] M. Wang, Y. Yu, X. Wu, S. Li, Polymer 45 (2004) 1253.
[18] G. Li, P. Li, C. Zhang, Y. Yu, H. Liu, S. Zhang, X. Jia, X. Yang, Z. Xue, S.K. Ryu, Compos. Sci. Technol. 68 (2008) 987.
[19] R.S. Dave, A.C. Loos, Processing of Composites, Hanser-Gardner Publications, Washington, DC, 2000.
[20] J.W. Park, S.C. Kim, Polym. Adv. Technol. 7 (1995) 209.
[21] P.A. Oyanguren, B. Aizpurua, M.J. Galante, J. Polym. Sci. Polym. Phys. 37 (1999) 2711.
[22] M.I. Giannotti, M.S. Solsona, M.J. Galante, P.A. Oyanguren, J. Appl. Polym. Sci. 89 (2003) 405.
[23] S. Ponceta, G. Boiteuxa, J.P. Pascaulta, H. Sautereaua, G. Seytrea, J. Rogozinskib, D. Kranbuehlb, Polymer 40 (1999) 6811.
[24] A. Bonnet, J.P. Pascault, H. Sautereau, Macromolecules 32 (1999) 8524.
[25] E.A. Mertzel, D.R. Perchak, W.M. Ritchey, J.L. Koenig, Ind. Eng. Chem. Res. 27 (1988) 580.
[26] M.L. Huang, J.G. Williams, Macromolecules 27 (1994) 7423.
[27] K.C. Cheng, W.Y. Chiu, Macromolecules 26 (1993) 4665.
[28] A. Agrawal, D.R. Uhlmann, Polymer 32 (1991) 290.
[29] S.C. Kim, M.B. Ko, W.H. Jo, Polymer 36 (1995) 2189.
[30] C.G. Delides, D. Hayward, R.A. Pethrick, A.S. Vatalis, J. Appl. Polym. Sci. 47 (1993) 2037.
[31] S. Bandyopadhyay, Mater. Sci. Eng. A 125 (1990) 157.
[32] H.S. Min, S.C. Kim, Polym. Bull. 42 (1999) 221.